molecular distillation at 0.05 mmHg: ^1H NMR ($CDCl_3$/TMS) δ 8.25 (m, 1 H, ArH), 7.50 (m, 2 H, ArH), 7.28 (m, 1 H, ArH), 5.64 (d, 2 H, olefinic protons, $J = 2$ Hz), 2.89 (d, 2 H, CH_2SeAr, $J = 6$ Hz), 2.45–1.70 (br m, 6 H, cyclohexenyl methylene protons), 1.42 (m, 1 H, methine proton); ^{13}C NMR ($CDCl_3$) δ 133.32, 129.05, 126.90, 126.31, 125.44, 125.10, 32.97, 32.80, 32.14, 29.07, 24.62; IR (neat) 3020 (olefinic CH), 2960, 2920, 2840 (aliphatic CH), 1655 (olefinic CC), 1590 (Ar), 1565, 1515 ($ArNO_2$), 1450, 1435, 1330 ($ArNO_2$), 1305, 1250, 1230, 1215, 1170, 1145, 1095, 1050, 1035, 955, 915, 850, 780, 725, 700, 660 cm^{-1}. Exact mass mol wt. Calcd for $C_{13}H_{15}O_2NSe$: 297.0266. Found: 297.0249. Anal. Calcd for $C_{13}H_{15}O_2NSe$: C, 52.71; H, 5.10; N, 4.73. Found: C, 52.77; H, 5.30; N, 4.60.

4-Methylenecyclohexene. A solution composed of 500 mg (1.69 mmol) of 1-[((2-nitrophenyl)seleno)methyl]-3-cyclohexene in 20 mL of tetrahydrofuran was added to a solution of 505 mg (2.36 mmol) of sodium periodate in 20 mL of a methanol/water (7:3) mixture and stirred at room temperature for 24 h. Pentane and saturated aqueous sodium bicarbonate solution were added. The pentane layer was washed with brine, dried (anhydrous sodium sulfate/potassium carbonate), filtered, and concentrated. The residue was subjected to preparative GLC (10% SE-30, 80 °C), and 50 mg of 4-methylenecyclohexene was isolated. The ^1H NMR spectrum of 4-methylenecyclohexene was identical with that reported by Babad et al.:[50] ^1H NMR ($CDCl_3$/TMS) δ 5.67 (d, 2 H, olefinic CH, $J = 1.5$ Hz), 4.73 (br s, 2 H, vinyl CH_2), 2.76 (m, 2 H, doubly allylic CH_2), 2.24 (m, 4 H, allylic CH_2's).

***cis*-Bicyclo[4.1.0]heptane (40).** The method utilized in the synthesis of *cis*-bicyclo[4.1.0]hept-3-ene was also used for the synthesis of **40** according to a modification of the procedure by Paquette.[14]

Acknowledgment. We are indebted to the National Science Foundation for a grant that supported this investigation.

Registry No. 9, 84194-54-7; **10**, 119146-73-5; **11**, 101934-24-1; **13**, 25126-93-6; **14**, 53389-31-4; **15**, 84194-49-0; **16**, 119146-74-6; **17**, 84194-50-3; **18**, 84194-51-4; **19**, 84194-52-5; **20**, 84194-53-6; **21**, 71655-17-9; **22**, 59533-63-0; **23**, 101934-25-2; **24**, 101934-26-3; **25**, 119239-81-5; **26**, 101934-27-4; **27**, 119146-75-7; **28**, 119239-82-6; **29**, 16554-83-9; **30**, 119146-76-8; **31**, 119146-77-9; **32**, 36168-41-9; **33**, 6802-78-4; **34**, 119146-78-0; **35**, 119239-83-7; **36**, 70095-44-2; **37**, 70095-43-1; **38** (isomer 1), 119146-72-4; **38** (isomer 2), 119146-79-1; **39**, 110-83-8; **40**, 286-08-8; **43**, 26325-89-3; **44**, 100-40-3; **45**, 4054-38-0; CH_2I_2, 75-11-6; Na_2S, 1313-82-2; $[Rh(CO)_2Cl]_2$, 14523-22-9; $[Rh(COD)Cl]_2$, 12092-47-6; 1-cyanonaphthalene, 86-53-3; triflic acid, 1493-13-6; *p*-toluenesulfonic acid, 104-15-4; 1-methylcyclohexa-1,4-diene, 4313-57-9; toluene, 108-88-3; methyl cyclohexenecarboxylate, 6493-77-2; 1-[((2-nitrophenyl)seleno)methyl]-3-cyclohexene, 88090-53-3; 1-(hydroxymethyl)-3-cyclohexene, 1679-51-2; *o*-nitrophenyl selenocyanate, 51694-22-5; 4-methylenecyclohexene, 13407-18-6; 1-ethyl-1,4-cyclohexadiene, 19841-74-8; 4-ethylene-1-cyclohexene, 16631-66-6; 4-isopropylene-1-cyclohexene, 119182-77-3.

---

[50] Babad, H.; Flemon, W.; Wood, J. B., III *J. Org. Chem.* **1967**, *32*, 2871.

Photodimerization of Isophorone in Supercritical Trifluoromethane and Carbon Dioxide

Bruce J. Hrnjez,[1] Anil J. Mehta,[2] Marye Anne Fox,*[,1] and Keith P. Johnston*[,2]

Contribution from the Departments of Chemistry and Chemical Engineering, University of Texas at Austin, Austin, Texas 78712. *Received August 30, 1988*

Abstract: An examination of the regio- and stereoselectivity for the photodimerization of isophorone in both supercritical CHF_3 and CO_2 as a function of pressure is presented. This selectivity is discussed in terms of solvent polarity and differential solvent reorganization. The stereoselectivity is influenced mostly by solvent reorganization, and the regioselectivity is influenced by both solvent polarity and solvent reorganization. Differential solvent reorganization is shown to exert the dominant effect on the selectivity, and the viability of a supercritical medium as a mechanistic probe is thereby demonstrated.

In their regions of high compressibility, supercritical fluids[3,4] are powerful tools for probing solvent effects in a wide variety of chemical systems.[5-13] Normally, solvent effects in chemical reactions are probed via a change in solvent or a large change in temperature, both of which amount to major perturbations on the particular system studied. The beauty of a supercritical fluid is that a minor perturbation, i.e., a small change in pressure in the vicinity of the critical point, affords a large change in the density-dependent bulk solvent properties such as dielectric constant and viscosity.

Supercritical fluids are well-known for their applications in separations technology.[3] Despite their obvious potential utility, supercritical fluids have only recently been used as media for the study of ground-state chemical reactions.[5-13] Moreover, photochemical and photophysical phenomena in such media are largely unexplored. Squires[14] briefly examined the photochemical cis–trans isomerization of stilbene in CO_2. Leffler[15] studied the photochemical cis to trans relaxation of 4-(diethylamino)-4′-nitroazobenzene in CO_2. In the photophysical realm, Mataga[16] and Kajimoto[17] examined exciplex fluorescence and charge-transfer-state formation, respectively, in CHF_3.

As part of an effort to understand both the behavior of supercritical fluids on a molecular level and the fundamental nature

---

[1] Department of Chemistry.

[2] Department of Chemical Engineering.

[3] McHugh, M.; Krukonis, V. *Supercritical Fluid Extraction*; Butterworths: Boston, 1986.

[4] Moore, W. J. *Physical Chemistry*; Prentice-Hall: Englewood Cliffs, NJ, 1972; pp 23–25.

[5] Subramaniam, B.; McHugh, M. A. *Ind. Eng. Chem. Process Des. Dev.* **1986**, *25*, 1.

[6] Flarsheim, W. M.; Tsou, Y.; Trachtenberg, I; Johnston, K. P.; Bard, A. J. *J. Phys. Chem.* **1986**, *90*, 3857.

[7] Kim, S.; Johnston, K. P. *Ind. Eng. Chem. Res.* **1987**, *26*, 1206.

[8] Johnston, K. P.; Haynes, C. *AIChE J.* **1987**, *33*, 2017.

[9] Kim, S.; Johnston, K. P. *Chem. Eng. Comm.* **1987**, *63*, 49.

[10] Flarsheim, W. M.; Johnston K. P.; Bard, A. J. *J. Electrochem. Soc.*, in press.

[11] Flarsheim, S. M.; Johnston, K. P.; Bard, A. J. *J. Phys. Chem.*, submitted for publication.

[12] Peck, D.; Mehta, A. J.; Johnston, K. P. *J. Phys. Chem.*, submitted for publication.

[13] Alexander, G. C.; Paulaitis, M. E. *Pure Appl. Chem.* **1987**, *59*, 61.

[14] Aida, T.; Squires, T. G. In *Supercritical Fluids, Chemical and Engineering Principles and Applications*; ACS Symposium Series 329; Paulaitis, M. E., Ed.; American Chemical Society: Washington, DC, 1987.

[15] Sigman, M. E.; Leffler, J. E. *J. Org. Chem.* **1987**, *52*, 3123.

[16] Okada, T.; Kobayashi, Y.; Yamasa, H.; Mataga, N. *Chem. Phys. Lett.* **1986**, *128*, 583.

[17] Kajimoto, O.; Futakami, M.; Kobayashi, T.; Yamasaki, K. *J. Phys. Chem.* **1988**, *92*, 1347.

0002-7863/89/1511-2662$01.50/0

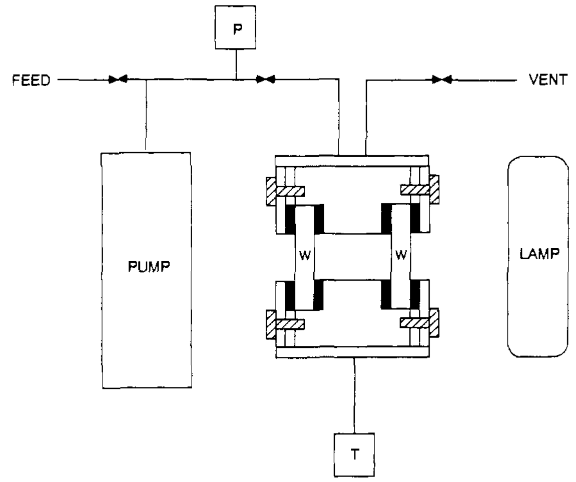

Figure 1. Schematic diagram of apparatus for photochemistry in supercritical media. T, temperature indicator-controller; P, pressure indicator; W, sapphire window.

of solvent effects in general, we studied the photodimerization of a cyclic enone, isophorone **1**, in both supercritical CHF_3 and CO_2 as a function of pressure. We selected enone **1** for study because the regiochemical outcome of its [2 + 2] photodimerization is highly solvent dependent. Chapman[18] reported that the ratio of head-to-head dimer (**2**) to total head-to-tail dimers (**3** + **4**) changes from 1:4 to 4:1 when the solvent is changed from cyclohexane to methanol (see eq 1). The less polar medium favors the less polar head-to-tail dimers **3** and **4**, whereas the more polar medium favors the more polar head-to-head dimer **2**. We hoped, therefore, to effect a change in product selectivity as a function of pressure in supercritical media, and we now report the results of our investigation.

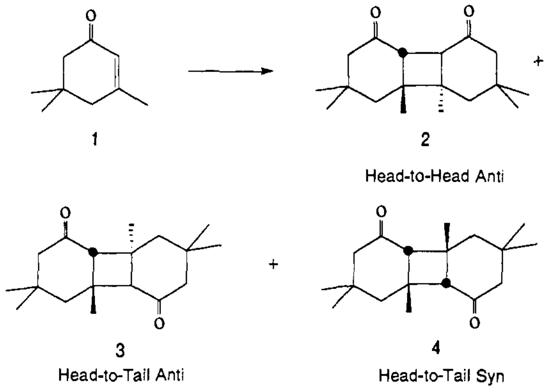

(1)

Experimental Section

Isophorone (Aldrich, 98%) was vacuum distilled to a purity of >99%. Instrument-grade CO_2 (Linde, >99.5%) was used as received. CHF_3 (Linde, >98%) was deoxygenated by freeze-thaw vacuum techniques to a molecular oxygen concentration of <10 ppm. Photoproduct analyses were performed on a Hewlett-Packard 5890 gas chromatograph (GC) equipped with a capillary column (HP-1, 25-m length × 0.32-mm i.d., 0.52-mm film thickness).

Irradiation. A cylindrical stainless steel (316) cell (1.75-cm i.d., 6.35-cm o.d., 1.0-cm internal length, 2.5-mL volume), fitted with two sapphire windows (2.5-cm diameter, 1.0-cm thickness), was used as a photoreactor (Figure 1). The temperature of the cell was monitored with a platinum resistance thermometer (Omega) and controlled to within ±0.1 °C with a temperature controller (Omega 6000 series), two cartridge heaters, and a circulating-water coolant jacket. A syringe pump (High Pressure Equipment, 30-mL capacity) was used to introduce solvent and to control the pressure. The pressure was measured to ±0.1% accuracy with a digital pressure gauge (Heise Model 710A).

The light source was a 450-W medium-pressure Hg lamp (Hanovia) fitted with a Pyrex filter. The initial concentration (0.06 M) of enone **1**, and the irradiation time (12 h) were held constant for all runs in both CHF_3 and CO_2. Irradiations in CO_2 were performed at a constant temperature of 38 °C at several pressures from 89.0 to 281.4 bar. Irradiations in CHF_3 were performed at a constant temperature of 34.5 °C at several pressures from 57.6 to 482.8 bar.

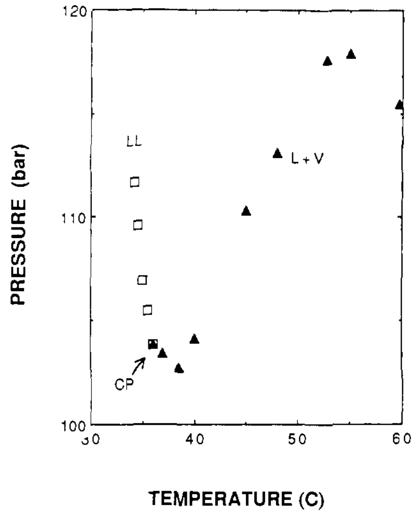

Figure 2. Phase diagram for binary enone **1**/CO_2 system. CP denotes critical point. Filled triangles define dew point or liquid + vapor (L + V) curve; open squares define liquid-liquid (LL) curve.

Typically, the cell was repeatedly pressurized (>10 bar) with the desired solvent and then vented in order to remove air. The enone **1** was then introduced via syringe through an open port under a positive pressure of the solvent. The cell was heated to the required temperature, solvent was introduced, and the pressure was adjusted. After irradiation, the cell contents were slowly bubbled through a methylene chloride tap, and the cell was rinsed with several portions of methylene chloride. The combined trap solvent and cell washings were analyzed by GC (temperature gradient from 100 to 250 °C) for the distribution of photoproducts **2**, **3**, and **4**. Peak assignments were made with reference to samples obtained from irradiation in methanol, and the regiochemistries of **2**, **3**, and **4** were previously determined.[18,19] The stereochemistry of anti head-to-head dimer **2** was assigned via its crystal structure.[20] The stereochemistry of anti head-to-tail dimer **3** was previously determined via its crystal structure.[21] By default, the stereochemistry of head-to-tail dimer **4** was assumed to be syn.

Phase behavior. A cylindrical stainless steel (316) variable-volume view cell (1.75-cm i.d. × 5.0-cm o.d., 9.2-cm internal length), fitted with a stainless steel (316) piston (2.5-cm length) and a sapphire window (2.5-cm diameter, 1-cm thickness) on the front face, was used to study the pressure-temperature phase behavior. The volume, and hence the pressure, in the sample compartment was varied by movement of the piston, which was controlled by hydrostatic pressure on the side of the piston opposite the sample compartment. The sample compartment pressure was measured to within 0.1% (Sensotec Model GM with submersible transducer), and the temperature was measured with a platinum resistance thermometer (Omega) coupled to a temperature controller (Omega 6000 series). Temperature control was achieved by submersion of the cell in a constant-temperature water bath (Haake circulator). The sample was magnetically stirred.

Isophorone **1** (0.35 mol % for CO_2 and 6.4 mol % CHF_3) was loaded into the sample compartment, followed by the solvent (measured by weight). At each temperature, the mixture was brought to a single phase by increasing the pressure, which was then slowly decreased until the onset of a second phase was observed (sudden appearance of cloudiness). Stirring was stopped, and a meniscus developed either at the top or bottom of the window. A meniscus at the top indicated the onset of vaporization (bubble point), while a meniscus at the bottom indicated the onset of condensation (dew point). Repeated measurements reduced the uncertainty in pressure to <0.5 bar. In the CHF_3 system, the location of the critical point was apparent from the intersection of the bubble point and dew point curves, and confirmed by the observation of opalescence. In the CO_2 system, the phase diagram (Figure 2) is complicated by a

---

[18] Chapman, O. L.; Nelson, P. J.; King, R. W.; Trecker, D. J.; Griswold, A. *Rec. Chem. Prog.* **1967**, *28*, 167.

[19] Fox, M. A.; Cardona, R.; Ranade, A. C. *J. Org. Chem.* **1985**, *50*, 5016.

[20] Available as supplementary data. We thank V. Lynch of the University of Texas at Austin for determination of the X-ray crystal structure of **2**.

[21] Cardona, R. Ph.D. Dissertation, University of Texas at Austin, 1987.

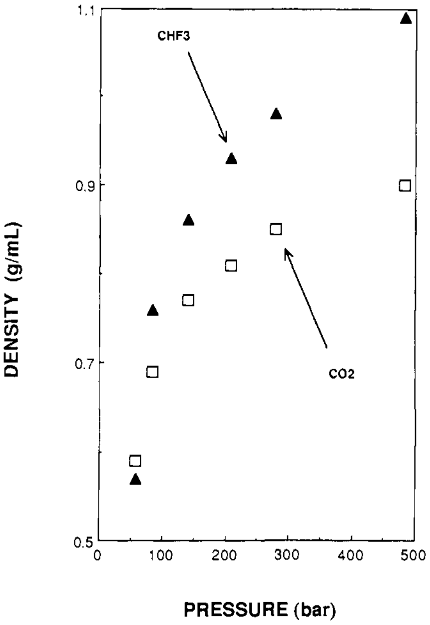

Figure 3. Variation in density with pressure for initial reaction mixtures of 0.06 M isophorone **1** in CHF_3 (34.5 °C) and CO_2 (38 °C).

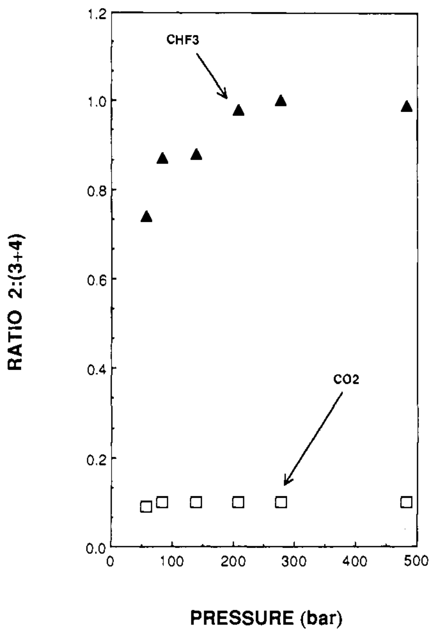

Figure 4. Variation in ratio of photoproducts head-to-head *anti*-**2** to total head-to-tail **3** plus **4** with pressure for irradiation of 0.06 M isophorone **1** in CHF_3 (34.5 °C) and CO_2 (38 °C).

Table I. Photoproduct Selectivity in CHF_3 as a Function of Pressure

pressure, bar	density, g/mL	2:(3+4)	3:4	2:4	2:3
57.6	0.57	0.74	2.56	2.65	1.04
83.5	0.76	0.87	2.90	3.40	1.17
139.0	0.86	0.88	3.24	3.71	1.15
206.9	0.93	0.98	3.16	4.08	1.29
277.6	0.98	1.00	3.32	4.32	1.30
482.8	1.09	0.99	3.83	4.76	1.24

Table II. Photoproduct Selectivity in CO_2 as a Function of Pressure

pressure, bar	density, g/mL	2:(3+4)	3:4	2:4	2:3
89.0	0.59	0.09	2.00	0.27	0.14
106.2	0.69	0.10	2.30	0.32	0.14
140.0	0.77	0.10	2.61	0.38	0.15
173.8	0.81	0.10	3.12	0.41	0.13
209.7	0.85	0.10	3.63	0.44	0.12
281.4	0.90	0.10	3.95	0.49	0.12

liquid–liquid (LL) phase separation at temperatures below the curve indicated LL. The liquid plus vapor (L + V) or dew point curve ends at the mixture critical point, where opalescence was observed. At pressures above this dew curve, only a single fluid phase is present. This dew curve lies in the retrograde region because dew condenses from the dense fluid as the pressure is decreased.[22] It is likely that there is a small three-phase liquid–liquid–vapor (LLV) curve between the LL curve and the mixture critical point. Since is was not relevant to our purpose, we did not explore this region. The critical values at 0.35 mol % enone **1** in CO_2 are T_c = 37 °C and P_c = 103 bar. The critical values for 0.35 mol % **1** in CHF_3 (extrapolated from a 6.4 mol % determination) are T_c = 34 °C and P_c = 56.5 bar. Phase behavior studies were performed at constant mole percent, but nonconstant volume and therefore nonconstant molarity. The photochemical experiments were performed at constant volume and therefore constant molarity, but nonconstant mole percent. The phase behavior at 0.35 mol % is a necessary approximation of the critical behavior in our fixed-volume photochemical system.

Results

We elected to study the photodimerization of isophorone **1** at a concentration of 0.06 M for several reasons. First, a low concentration mitigates ambiguities arising from self-solvation, or clustering, of **1** in the ground state but is sufficiently high for an effective bimolecular reaction. Second, operation at substantially higher concentrations necessitates operation at substantially higher temperatures. For example, the critical temperature for 0.5 M **1** in CHF_3 is about 70 °C. A low concentration minimizes the possibility of introducing alternative excited-state manifolds at elevated temperatures. Last, a low concentration ensures that the photodimerization proceeds only via the triplet of **1**. At 0.06 M **1**, the bimolecular photodimerization from the short-lived singlet of **1** cannot compete effectively with rapid intersystem crossing to the triplet. Coumarin is known[23] to give photodimers of different stereochemistry from the excited singlet and triplet states.

Both Squires[14] and Leffler[15] studied unimolecular phenomena in supercritical CO_2. Such studies can be performed at high dilution and therefore circumvent the problem of a change in the critical properties from those of the pure solvent. In contrast, we studied a bimolecular photochemical process. At the 0.06 M concentration required for an efficient bimolecular reaction, the critical properties of the binary systems vary from those of the pure fluids. We therefore studied the phase behavior of **1** in both CO_2 and CHF_3 in order to ensure that we were operating in a single phase and in the respective regions of high compressibility. Figure 2 depicts the phase behavior for the binary **1**/CO_2 system.[22] Determination of the initial reaction mixture densities at each pressure in both solvents confirmed that we operated in regions of high compressibility (Figure 3). Briefly, the amount of solvent loaded into the reactor was measured volumetrically with the vernier scale of the syringe pump, and the densities of the pure fluids were used to convert the volumes to weight.

We irradiated isophorone **1** in CO_2 (38 °C) and in CHF_3 (34.5 °C) as a function of pressure. The results of our irradiations, in terms of product ratios, are shown in Tables I and II and are depicted graphically in Figures 4–7. Reactions times were held constant at 12 h and product compositions were determined by GC. Because of the low initial concentration of enone **1**, the total yield of products **2**, **3**, and **4** in all runs was about 2% (based on **1**).[24]

---

(22) Prausnitz, J. M.; Lichtenthaler, R. N.; de Azeuedo, E. G. *Molecular Thermodynamics of Fluid Phase Equilibria*; Prentice-Hall: Englewood Cliffs, NJ, 1986.

(23) Hammond, G. S.; Stout, D. A.; Lamola, A. A. *J. Am. Chem. Soc.* **1964**, *86*, 3103.

(24) Total disappearance of **1** averaged about 20%, the bulk of which was accounted for by photoisomerization of **1** to an unidentified monomeric product. This same side product was observed in both CHF_3 and CO_2. Some unidentified dimeric photoproducts were formed, presumably arising from photoisomerized **1**. These side products did not interfere with identification or analysis of the photoproducts of interest.

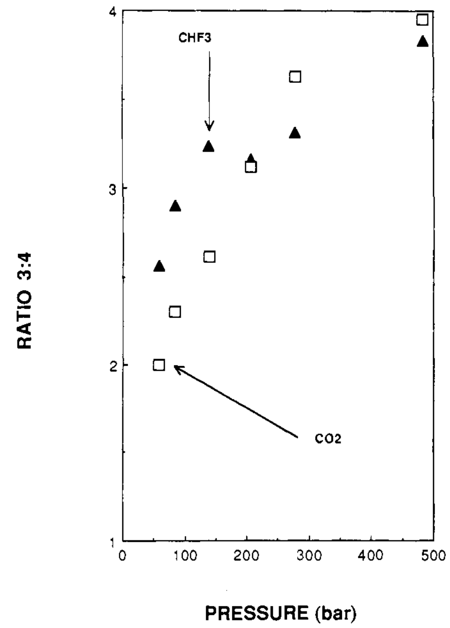

Figure 5. Variation in ratio of photoproducts head-to-tail *anti*-**3** to head-to-tail *syn*-**4** with pressure for irradiation of 0.06 M isophorone **1** in CHF_3 (34.5 °C) and CO_2 (38 °C).

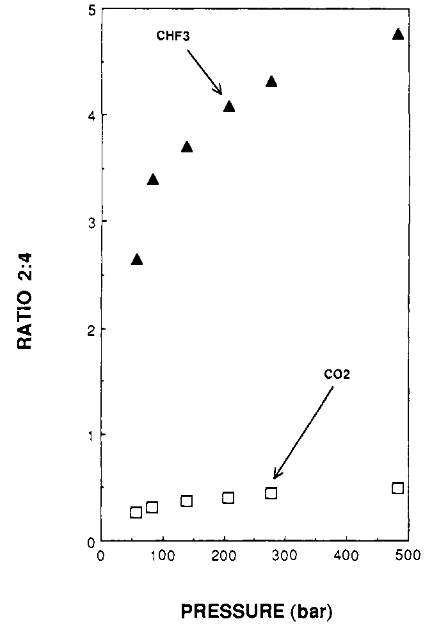

Figure 6. Variation in ratio of photoproducts head-to-head *anti*-**2** to head-to-tail *syn*-**4** with pressure for irradiation of 0.06 M isophorone **1** in CHF_3 (34.5 °C) and CO_2 (38 °C).

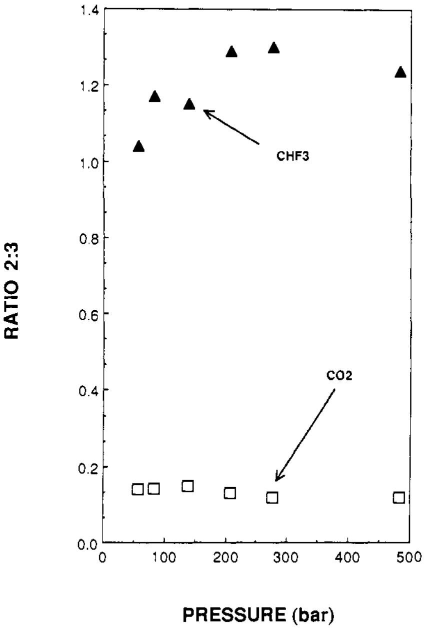

Figure 7. Variation in ratio of photoproducts head-to-head *anti*-**2** to head-to-tail *anti*-**3** with pressure for irradiation of 0.06 M isophorone **1** in CHF_3 (34.5 °C) and CO_2 (38 °C).

Discussion

The previously observed[18] photodimer regioselectivity **2**:(**3** + **4**) in common liquid solvents (vide supra) was rationalized on the basis of the probable transition-state dipole moments leading to **2**, **3**, and **4**. The dipole moment of isophorone **1** is 3.99 D, while that of the head-to-head dimer **2** is 5.08 D. The dipole moments of the head-to-tail dimers **3** and **4** are 1.03 and 1.09 D, respectively.[18] If the photodimerization proceeds via a late, and therefore product-like, transition state,[25] then the respective transition-state polarities may be approximated by those of the products. Therefore, a polar solvent should favor the dipole moment increase from **1** to **2**, whereas a nonpolar solvent should favor the dipole moment decrease from **1** to **3** and **4**.

In accord with liquid solvent chemistry,[18,19] the more polar dimer **2** was a major product in the polar CHF_3 and a relatively minor product in the nonpolar CO_2 (Figure 4). Since we had access to a modest change in the dielectric constant with pressure for CHF_3 (2.5 to 8.4),[26] we were able to effect a modest change in the regioselectivity for head-to-head versus head-to-tail isomers of 0.74 to 1.0. In contrast, only a relatively small change in the dielectric constant of the CO_2 medium was available (1.34 to 1.54),[26] and this was reflected in a negligible change in regioselectivity.

The regioselectivities **2**:(**3** + **4**) in 1.4-dioxane (2.209 D) and neat isophorone **1** (3.99 D) are 0.44 and 0.63, respectively.[18] We might therefore have expected a greater change in the regioselectivity with the greater than threefold change in CHF_3 dielectric constant. In highly compressible supercritical fluids, the solvent is strongly attracted to the solute and partial molar volumes may reach thousands of mL/mol negative.[27] The degree of clustering of solvent in the local environment of solute was determined spectroscopically and explained theoretically.[7,11] Because of this clustering, the local dielectric constants at the lower pressures are much larger than the bulk values. At higher pressures, the compressibility of the solvent decreases as it becomes more "liquid-like" so that the local dielectric constant is nearer the bulk value. As a result, the change in the local dielectric is smaller than the change in the bulk dielectric with pressure, and the change in the selectivity is therefore smaller than might be expected. However, the CHF_3 experiment is a more direct test of the effect of a change in solvent polarity than is a comparison of results obtained in dioxane and neat isophorone **1**. Surely, the difference between solvation in dioxane and self-solvation in the neat reactant is enough to obscure a true test of the change in polarity on regioselectivity. Specific solvent effects do not change with pressure in supercritical media.

It was also reported[18] that the head-to-tail dimers **3** and **4** were formed in approximately equal quantities under all conditions studied in normal liquid solvents. We were therefore intrigued to find that dimer **3** was favored markedly and that the ratio of **3**:**4** was a distinct function of pressure (Figure 5) in both CO_2 (from 2.0 to 4.0) and CHF_3 (from 2.6 to 3.8).

We contend that the relative degree of solvent reorganization required for dimerization leading to the anti (**3**) versus syn (**4**) configurations (Figure 8) accounts for this unexpected result. Intuitively, it is apparent that the reactive enone species **1** need

---

(25) le Noble, W. J.; Tamura, K. *Tetrahedron Lett.* **1977**, 495.

(26) Mehta, A. Masters Thesis, University of Texas at Austin, 1988.

(27) Eckert, C. A.; Zeiger, D. H.; Johnston, K. P.; Kim, S. *J. Phys. Chem.* **1986**, *90*, 2738.

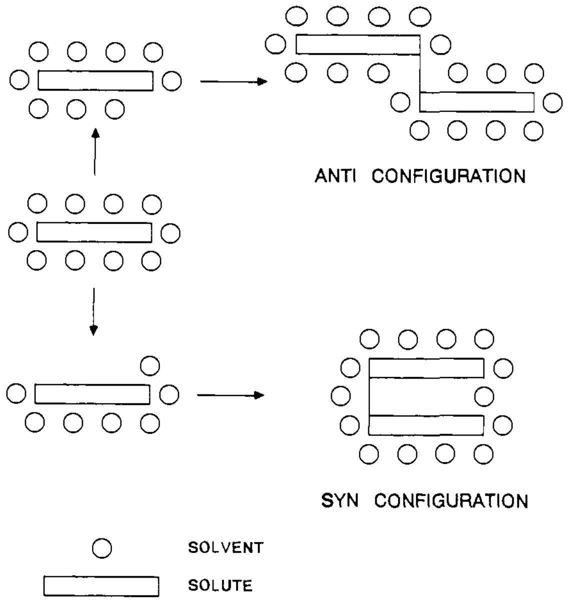

Figure 8. Schematic representation of relative solvent reorganization required for photodimerization leading to the syn versus anti configurations. Rectangles represent the plane of the cyclohexyl rings and circles represent solvent molecules.

undergo a small degree of "desolvation" in order to effectively dimerize to an anti configuration relative to the large degree of desolvation (nearly half the solvent sphere) required for effective dimerization to the syn configuration. This relative degree of desolvation required for dimerization to anti or syn should be reflected in the relative activation barriers leading to **3** or **4**. Clearly, steric congestion in the transition state leading to **4** also contributes to preferential formation of **3**, but cannot account for the variation of **3**:**4** with pressure. Therefore, the product distribution **3**:**4** at a given pressure is, at least partially, a kinetic effect resulting from differential solvent reorganization.

This concept is also consistent with the observation that the ratio of **3**:**4** (anti:syn) increases with pressure. At low pressures where the gas is ideal, the effect of solvent reorganization should be small. As pressure is increased, the solvent density increases and solvent reorganization becomes progressively more important. As a result, the differential in reorganization leading to the syn and anti configurations becomes larger and the ratio of **3**:**4** increases.

An alternative and complementary view is based on a thermodynamic effect or rate constants.[8] We assume that the solute–solvent attractive forces are similar for the two transition states leading to **3** and **4** because the dipole moments of these products are nearly equal. Therefore, the thermodynamic effect is most likely dominated by solute–solvent repulsive forces because of the size difference between the two isomers. Since the anti configuration (**3**) requires a smaller cavity in the solvent, it is favored thermodynamically over the syn configuration (**4**) with an increase in pressure.

Our supposition that *anti*-**3** requires a smaller cavity is reinforced by MM2[28] calculations of the relative solvent accessible surface areas[29] for **3** and **4**. Representatively, in CO_2 (radius 2.56 Å) the values are 345.9 and 314.6 Å^2 for **3** and **4**, respectively. The difference arises from the fact that the syn configuration has a cleft between the planes of the two cyclohexyl rings from which solvent is excluded. In effect, *syn*-**4** with its excluded volume is larger than *anti*-**3**.

Table III. Summary of Relative Contributions of Solvent Reorganization and Polarity Effects to the Increase in Product Ratios **3**:**4**, **2**:**3**, and **2**:**4** with Increasing Pressure

product ratio	selectivity type	reorg effect	polarity effect
3:**4**	stereo	large	small
2:**3**	regio	small	large
2:**4**	stereo + regio	large	large

The ratio **2**:**4** demonstrates a dual dependence on both solvent reorganization and solvent polarity as a function of pressure (Figure 6). Both factors cause this ratio to increase. The polarity factor (favoring head-to-head **2** over head-to-tail **4**) works in concert with the reorganization factor (favoring *anti*-**2** over *syn*-**4**), but their relative contributions are not readily discernible. In contrast, the solvent reorganization factor plays a negligible role in anti–anti ratio **2**:**3** (Figure 7) because of their similarity in molecular configurations. In fact, the anti head-to-head (**2**) versus anti head-to-tail (**3**) pressure dependence is perhaps the purest revelation of a solvent polarity effect in the overall product selectivity. Furthermore, the aforementioned ratio **3**:**4** serves to isolate the solvent reorganization effect, while the ratio **2**:(**3** + **4**) is an inseparable admixture of the two solvent effects. Table III summarizes our observations.

Overall, the ratio **2**:**4** changes by a factor of 1.8 in both CHF_3 and CO_2, whereas the ratio **2**:**3** changes by a factor of only 1.2 in CHF_3 and is virtually invariant in the nonpolar CO_2. We must conclude that differential solvent reorganization plays the dominant role in product selectivity for the photodimerization of isophorone **1**.

Conclusion

In supercritical media, the photodimerization of isophorone **1** is a powerful model for investigating both solvent reorganization effects (solute–solvent repulsive interactions) and solvent polarity effects (solute–solvent attractive interactions). We found that the stereoselectivity is influenced mostly by solvent reorganization and that the regioselectivity is influenced by both solvent polarity and solvent reorganization. The solvent reorganization factor has a larger pressure effect on stereoselectivity than the polarity factor has on regioselectivity. Hence, the solvent reorganization factor is dominant.

The control over regio- and stereoselectivity in the photodimerization of **1** demonstrates the potential utility of supercritical fluids as reaction media and their viability as mechanistic probes. When a sufficient knowledge base is developed, supercritical fluids could become a tool for the synthetic organic chemist. Finally, the present study provides a useful qualitative insight into the behavior of supercritical fluids on a molecular level and a refinement of our understanding of the details of the photodimerization of cyclic enones.

Acknowledgment. We thank the donors of the Petroleum Research Fund, administered by the American Chemical Society, for partial support of this research (K.P.J.). We also gratefully acknowledge support from the National Science Foundation (Grant No. CHE-8509314 (M.A.F.)) and from the Separations Research Program at the University of Texas.

Registry No. **1**, 78-59-1; **2**, 72173-01-4; **3**, 28171-68-8; **4**, 72120-74-2.

Supplementary Material Available: A summary of data collection and refinement, tables of atom coordinates, thermal parameters, and bond distances and angles, and a figure showing the atom-labeling scheme for **2** (14 pages); structure factors for **2** (17 pages). Ordering information is given on any current masthead page.

---

[28] MM2 calculations were performed with C. Still's *MacroModel* program, version 1.5, Columbia University, 1987.

[29] Pearlman, R. S. *Physical and Chemical Properties of Drugs*; Marcel Dekker: New York, 1980.